Palaeontology
The Palaeontological Association
www.palass.org

[Palaeontology, Vol. 52, Part 6, 2009, pp. 1243–1256]

MORPHOLOGICAL CRITERIA FOR RECOGNISING HOMOLOGY IN ISOLATED SKELETAL ELEMENTS: COMPARISON OF TRADITIONAL AND MORPHOMETRIC APPROACHES IN CONODONTS

by DAVID JONES*,‡, MARK A. PURNELL* *and* PETER H. VON BITTER†

*Department of Geology, University of Leicester, Leicester LE1 7RH, UK; e-mails david.jones@bristol.ac.uk; map2@le.ac.uk
†Palaeobiology Division, Department of Natural History, Royal Ontario Museum, and Department of Geology, University of Toronto, Toronto, ON, Canada M5S 2C6; e-mail peterv@rom.on.ca
‡Current address: School of Biological Sciences, Monash University, Melbourne, VIC 3800, Australia

Typescript received 9 April 2008; accepted in revised form 15 March 2009

Abstract: Accurate hypotheses of primary homology are fundamental to many aspects of the systematics and palaeobiology of fossils. They are particularly critical for conodonts: virtually all areas of conodont research are underpinned by homology, yet the majority of conodont taxa are found only as disarticulated skeletal elements, and hypotheses of element homology are inferred from morphological comparisons with complete skeletons. This can cause problems in taxa where more than one location within the conodont skeleton is occupied by elements with similar morphology. In such cases, morphological comparisons can yield equivocal or erroneous hypotheses of homology of isolated elements. The Eramosa Lagerstätte of Ontario (Silurian, Wenlock) preserves both isolated skeletal elements and articulated conodont skeletons. The latter provide a topological context within which to test hypotheses of element homology and allow blind testing of qualitative discrimination of elements. When applied to P_1 and P_2 elements of *Wurmiella excavata*, this revealed inaccuracy and inconsistency in distinguishing these P element types. Standardised morphometric protocols were used to further test the efficacy of those characters used in traditional qualitative identification of P element homology, revealing that, individually, none of these characters provides an effective discriminator between P element types. Principal components and discriminant function analyses of ten 'traditional' morphological variables combined can distinguish P_1 from P_2 elements with a similar success rate to expert identification. Eigenshape and elliptic Fourier analyses of element outlines proved less effective at capturing shape differences that allowed for discrimination between P_1 and P_2 elements. Analysis of both traditional and outline data demonstrates that in some individuals P_1 and P_2 elements are morphologically distinct from one another, while in others they are almost indistinguishable. These results demonstrate that although qualitative assessments of homology can be prone to error, especially when undertaken by inexperienced researchers, the morphometric and analytical protocols used here provide effective additional tool for discriminating morphologically similar but non-homologous elements. These methods thus hold promise of broad application to other conodont taxa where identification of element homology in collections of isolated specimens is problematic.

Key words: homology, morphometrics, skeleton, conodont, *Wurmiella excavata*.

In common with work on all taxa with multicomponent skeletons, most aspects of conodont research depend on accurate hypotheses of primary homology between skeletal elements (Purnell and Donoghue 1998; Purnell *et al.* 2000). Element homology can only be identified unequivocally if skeletal architecture is fully understood (Barnes *et al.* 1979; Purnell 1993; Purnell *et al.* 2000), but this relies on uncommon articulated skeletons, preserved as natural assemblages and fused clusters. In collections of disarticulated elements, interpretations of element homology are largely reliant on morphological criteria (see Purnell and Donoghue 1998, and Purnell *et al.* 2000 for discussion). Because the conodont fossil record is dominated by disarticulated skeletal elements, problems can arise when elements occupying different locations within the conodont skeleton have similar morphologies.

Much conodont research is based on the elements that occupy the P_1 positions in the skeleton. Consequently, inaccurate identification of P element homology resulting from morphological similarity of P_1 and P_2 elements could have significant implications for our understanding of conodont palaeobiology and evolution and could

doi: 10.1111/j.1475-4983.2009.00915.x

(1) introduce false hypotheses of primary homology into cladistic and other phylogenetic analyses, potentially obscuring hypothesised relationships between taxa (Hawkins *et al.* 1997); (2) confound palaeoecological studies, by producing erroneous census counts from fossil samples (e.g. von Bitter and Purnell 2005) and masking true population structure; (3) limit our understanding of secular trends in ratios between different skeletal element types (Purnell and Donoghue 2005); (4) confuse patterns of morphological evolution occurring within each element location (Purnell 1993). For example, previous interpretations of changing apparatus structure through time, involving increases or decreases in the number of element types in the conodont skeleton (e.g. Merrill and Merrill 1974), probably result from morphologically similar elements occupying multiple locations within the apparatus.

The degree to which a given conodont taxon is susceptible to these potential biases differs according to the degree to which elements in different locations are morphologically distinct. Current hypotheses of the relationships between conodonts with morphologically complex elements suggest that during conodont evolution elements in different locations became more differentiated, with a large number of more basal taxa having morphologically similar elements in both P_1 and P_2 locations (Donoghue *et al.* 2008). In such cases, where a skeleton contains non-homologous but morphologically similar elements, it is clearly necessary to test hypotheses of conodont element homology and address these potentially significant biases. Here we report on a quantitative evaluation of alternative approaches to the recognition of homologies based on morphological criteria. Our data are derived from analysis of *Wurmiella excavata* (Branson and Mehl, 1933), a basal member of the Ozarkodinina (*sensu* Donoghue *et al.* 2008), a major clade of conodonts within which morphological differentiation of P elements increased markedly through time.

MATERIAL AND METHODS

Fossil material

Our specimens of *Wurmiella excavata* are from the fossil Konservat-Lagerstätte of the Eramosa Member (Silurian, Wenlock) on the Bruce Peninsula of southern Ontario, which preserves both articulated conodont skeletons and isolated elements (von Bitter and Purnell 2005; von Bitter *et al.* 2007). Several conodont species are represented in the Eramosa Lagerstätte but at localities B and D of von Bitter *et al.* (2007), the fauna is dominated by *W. excavata*. Examination of articulated *W. excavata* skeletons from the Eramosa Lagerstätte has revealed individuals whose P_1 and P_2 element morphologies appear remarkably similar

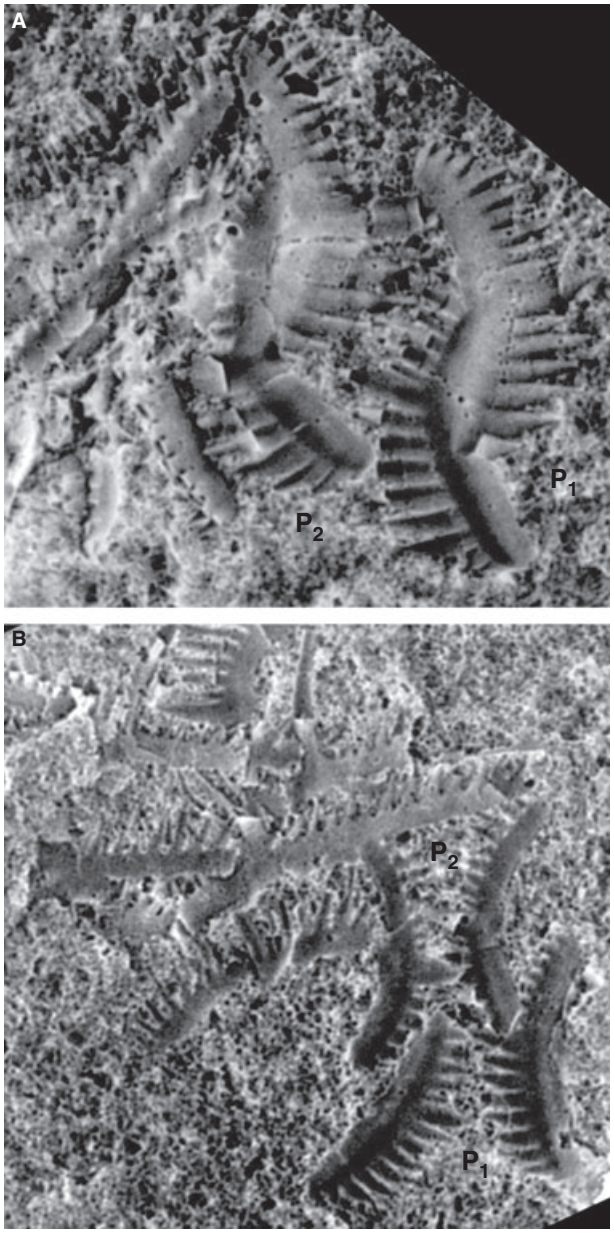

TEXT-FIG. 1. Light micrograph of (A) assemblage specimen ROM 59102 and (B) assemblage specimen ROM 59118 after ammonium chloride coating, illustrating morphological similarity of P_1 and P_2 elements in *W. excavata* from the Eramosa Lagerstätte.

(von Bitter and Purnell 2005; Text-fig. 1), something also hinted at in the first work to suggest these elements originally came from the same skeletal apparatus (Walliser 1964). Apparatuses collected by PvB were removed intact by him from bedding surfaces by undercutting with a small, carborundum-coated rotary blade on a Dremel electric tool. Following removal of all the articulated elements that could be located, the rocks were processed using standard buffered acid rock-dissolution techniques

(Jeppsson *et al.* 1999), with some additional processing stages required because of the bituminous nature of the Eramosa lithology. Most of the isolated elements and all of the articulated skeletons studied were prepared at the Royal Ontario Museum (ROM), Toronto and are housed there. Some additional isolated elements were recovered from two Eramosa sub-samples (of samples 01PB1 and 02PB1, see von Bitter and Purnell 2005) prepared in the micropalaeontology laboratories of the Department of Geology, University of Leicester. These sub-samples were predominantly carbonate lithologies. Frequency of elements within the sub-samples of 01PB1 and 02PB1, respectively, is approximately 96 and 50 per kg. Preservation of elements within the Eramosa Lagerstätte is good: isolated specimens generally have complete processes, and frequently retain intact denticles; elements preserved in apparatuses are generally fragmented, but fragments remain correctly juxtaposed in most cases. All elements are pale amber in colour. Further details of the lithology, preservation and biota of the Lagerstätte are given in von Bitter and Purnell (2005) and von Bitter *et al.* (2007).

Sixteen isolated P elements and 33 P elements from articulated skeletons were measured. Element images from which data were acquired are available from the authors. The number of elements measured from each skeleton varied according to element completeness and the number of elements not obscured by matrix; where feasible, matrix was carefully removed with a fine needle to better expose the elements (such preparation was recorded). Nevertheless, measuring elements within articulated skeletons remains difficult and sample sizes are consequently limited.

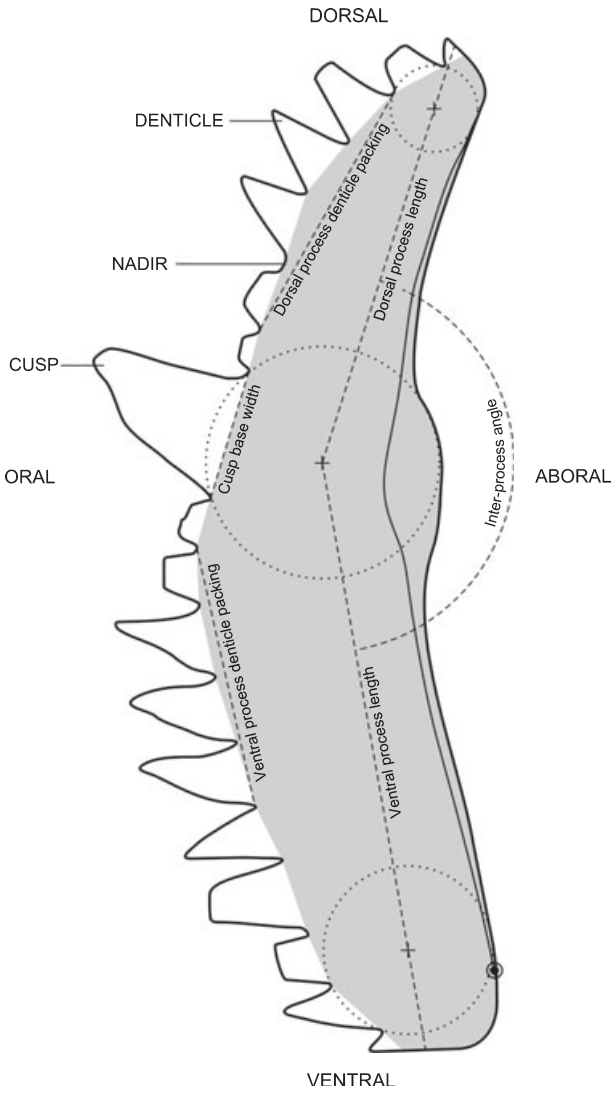

TEXT-FIG. 2. *W. excavata* P_1 element in 'lateral' (rostral-caudal) view. Measurements are identical for P_2 elements. Anchored circles are dotted. Dashed lines mark the measurements. Analysed outline indicated by grey shaded area. Starting point for outline digitisation indicated by ringed circle on ventral process.

Morphological measurements

Data were acquired using the morphometric protocols described in detail by Jones and Purnell (2007), using Media Cybernetics' ImagePro Plus© software. Text-figure 2 illustrates the measured variables and the biological anatomical notation (Purnell *et al.* 2000) used in this work. Denticle packing was represented by the length of a chord drawn between nadirs of the free tips of four denticles (the denticle packing line; see Text-fig. 2). In addition to those variables labelled in Text-figure 2, total length was calculated as the sum of the dorsal and ventral process lengths, and the number of denticles on each process was enumerated. The ratio of cusp base width to average denticle base width (the latter derived from denticle packing values for each process) was also calculated for dorsal and ventral processes, respectively. Although the use of ratios can be problematic (Atchley *et al.* 1976), the width of the cusp relative to denticle bases is frequently used in qualitative descriptions of conodont element morphology, and so is included for this reason. Raw data for the traditional measurements are tabulated in the Appendix; denticle packing is given in denticles per millimetre (the denticle packing line divided by four) to facilitate comparison with other studies.

To explore how shape differences not captured by the traditional measurements discriminated P_1 and P_2 elements, the shape of the P element 'lateral' profile (i.e. profile in rostro-caudal view) was examined using two outline techniques: eigenshape (ES) analysis (Lohmann 1983; Lohmann and Schweitzer 1990) and elliptic Fourier analysis (EFA: Giardina and Kuhl 1977; Kuhl and Giardina 1982; Ferson *et al.* 1985). Both approaches

standardise for size, revealing patterns of pure shape variation in the outlines analysed. Landmark-registered (extended) eigenshape analysis (MacLeod 1999) was not used because it emphasised fine details of the upper and lower margins, whereas for this particular study, we were interested in broader shape differences, which standard ES analysis captured more effectively.

Because denticle tips on conodont elements are frequently worn or lost through breakage, they were eliminated from the outline using a mask. This mask was drawn around the oral margin of the element forming a polygon with sides defined by chords connecting the nadirs between the free tips of the denticles, as shown in Text-figure 2. The aboral margin of the element formed the remainder of the outline. Elements without complete aboral margins were, therefore, excluded from the analyses, producing a sample size for the outline analyses of 38 isolated P elements and 17 P elements from articulated skeletons. No smoothing was performed on the outline, because it was not digitised finely enough to cause outline distortion (Haines and Crampton 2000); comparison of outlines with the original specimens they represent confirmed that the shapes are accurately represented.

Analysis – traditional measurements

Measurements for characters in univariate analysis were normally distributed (Shapiro–Wilk normality test, $W > 0.8$, $p > 0.05$ for all datasets). Patterns of covariation between articulated P_1 and P_2 elements in these characters were tested using Pearson correlation for linear measurements, conducted in PAST version 1.44 (Hammer *et al.* 2001), and circular-circular correlation for angular measurements conducted using Kovach Computing Service's Oriana version 2.

Principal components analysis (PCA) was applied to a dataset of isolated and articulated P elements, based on the ten traditional variables outlined in the previous section [PCA is a standard distribution-free ordination technique for reducing dimensionality in multivariate data and visualising and exploring data structure (Marcus 1990)]. Eight specimens of each P element type were sampled from articulated skeletons where both P element types were measured. A correlation matrix was used in the PCA, owing to the different units and scales of the measurements. Analysis was conducted in PAST version 1.44 (Hammer *et al.* 2001).

Analysis – outline data

TpsDig software version 1.37 (Rohlf 2003) was used to digitise element outlines to 200 Cartesian (x, y) coordinates, starting from the biologically and topologically homologous landmark at the ventral terminus of the basal cavity (see Jones and Purnell 2007 for discussion of homology within conodont elements in this context; see Text-fig. 2). Coordinate number was subsequently optimised in the eigenshape (ES) analysis by reducing the number of coordinates to the minimum required to reproduce the original outline to within an *a priori* tolerance criterion of 95 per cent. This also increases the efficiency of the analysis (MacLeod 1999). ES analysis was executed using MacLeod's (1999) standard eigenshape software (http://www.nhm.ac.uk/hosted_sites/paleonet/ftp/ftp.html) using the method discussed in MacLeod and Rose (1993) and MacLeod (1999). A covariance matrix was used, with shape functions mean centred so that shape variation is assessed as deviation from the mean shape and is spread over more axes.

Elliptic Fourier analysis (EFA) was conducted using Crampton and Haines' (1996) HSHAPE software (http://data.gns.cri.nz/paperdata/paper.jsp?id=78473). This program compensates for several shortcomings of EFA, particularly the generation of two redundant coefficients for each harmonic, the nonindependence of coefficients and the undue weighting of low order harmonics at the expense of higher order ones (for details, see Haines and Crampton 2000). Outlines were normalised for starting position and orientation using properties of the entire sample of outlines analysed. The appropriate number of harmonics to input to the subsequent multivariate analyses was determined using the Fourier power spectrum (Crampton 1995; Cronier *et al.* 1998): eight harmonics (represented by two coefficients each) summarised 99 per cent of the total variation, so harmonics nine and above were discarded. The primary patterns of variation captured by the EFA were extracted through PCA of the sixteen Fourier coefficients. A covariance matrix was used to preserve the scaling between variables (Crampton 1995). When producing end-member outlines using the inverse Fourier function (see Fourier results), the full 511 harmonics generated by the HSHAPE software were used, because the program re-samples outlines to operate at 1024 (x, y) coordinates.

Discriminant analysis

Linear discriminant function analysis (DFA; a multivariate technique for analysing potential groupings within a dataset) was used for examining element discrimination based on traditional and outline (eigenshape and elliptic Fourier) datasets. It was executed using SPSS version 16. Three separate DFAs were run: one each based on traditional data, eigenshape scores and elliptic Fourier coefficients. The robustness of each DFA was tested by

randomly removing a quarter of the elements of each type and ordinating these based on the discriminant function derived from analysis of the remaining elements. This validation test was conducted on datasets containing only P elements from articulated skeletons and thus of known P element type.

Because both traditional and outline data showed significant deviation from a multinormal distribution (Mardia multivariate skewness and kurtosis test, $p < 0.05$ for all datasets), a nonparametric multivariate analysis of variance (NPMANOVA) with a Bray–Curtis distance measure was used to test the null hypothesis that, based on the morphological data, P_1 and P_2 elements were not significantly different.

QUALITATIVE IDENTIFICATION OF ELEMENT HOMOLOGY

The accuracy of qualitative differentiation based on morphology alone was first tested in a blind experiment. Nineteen images of P element pairs from articulated skeletons were cropped (using Adobe Photoshop) so as to obscure their topological context, i.e. their true homology. These images were then presented to experienced conodont workers subscribed to the con-nexus listserver (http://www.conodont.net), who were asked to discriminate between P_1 and P_2 elements. Five people responded; of the 19 P element pairs, eight pairs were correctly identified by all workers, one pair was incorrectly assigned by all workers, and the remaining ten pairs had varying numbers of incorrect and uncertain identifications by different workers. Successful discrimination was related to individual experience: workers with Silurian experience and familiarity with *W. excavata* identified the most element pairs correctly, those whose main experience was with conodonts from other geological periods made the greatest number of inaccurate identifications. Although some workers correctly identified most elements, inconsistency between workers produced an overall success rate of 63 per cent.

In light of this between-worker inconsistency, the test was repeated using a further 12 images of isolated P elements, whose true homology was unknown, to test precision. This sample included specimens below the lower size range of the bedding-plane elements, to examine discrimination of younger individuals. A second group of five people responded, some of whom had taken part in the first test; 50 per cent of these isolated P elements were assigned differently by different workers. The incidence of inaccuracy and inconsistency among even experienced researchers suggests that novice workers might often incorrectly distinguish P_1 and P_2 elements within *W. excavata*. This bias will also affect other taxa in which P elements are less morphologically differentiated, for example in taxa within the Prioniodinina (Donoghue *et al.* 2008).

QUANTITATIVE IDENTIFICATION OF ELEMENT HOMOLOGY

P element discrimination based on traditional morphometric data

Because they preserve the elements of the conodont oropharyngeal apparatus in approximate life position (i.e. they preserve solid topological evidence of homology), the articulated skeletons from the Eramosa Lagerstätte offer a unique opportunity to further examine and address the difficulties of qualitative identification of element homology. By providing the largest available samples of *W. excavata* P elements in topological context, and therefore with known P_1 or P_2 locations within the skeleton, the material from the Eramosa Lagerstätte allows quantitative analysis of the morphological characters used by experienced workers to differentiate between P_1 and P_2 elements of *W. excavata* and testing of whether these characters provide an accurate and precise guide to distinguishing between them.

Morphological characters for analysis were chosen based on discussions with an expert in Silurian conodonts and on examination of illustrated specimens (Jeppsson 1969, fig. 3; 1974, plate 4; R. J. Aldridge, pers. comm. 2002). P element arching is commonly used to distinguish between P element types in *W. excavata*: P_1 elements are straight; P_2 elements are arched. Inter-process angles are used to capture this morphological information (see Jones and Purnell (2007) for methodology); straighter elements have larger inter-process angles, and arched elements have smaller inter-process angles. Cusp size is another frequently used character: P_1 elements have smaller cusps than P_2 elements. In complete elements, cusp height is generally used, but cusp height is often difficult or impossible to measure accurately because of breakage and potential wear at the tip. Yet breakage equally confounds qualitative assessment of cusp height and is often present in figured examples of *W. excavata* P_2 elements (e.g. Jeppsson 1969); in these cases, the cusp base must be used to provide an indication of cusp size. Because cusp base width can be readily measured, it is used here as an alternative to cusp height. Finally, relative process length was also examined; P_1 elements generally have ventral processes that are longer than dorsal, whereas in P_2 elements the dorsal process is the longer of the two.

Text-figure 3 plots each of these characters for a P_1 and a P_2 element in a number of articulated skeletons from the Eramosa Lagerstätte, to test the predicted patterns of covariation within the skeleton used to recognise

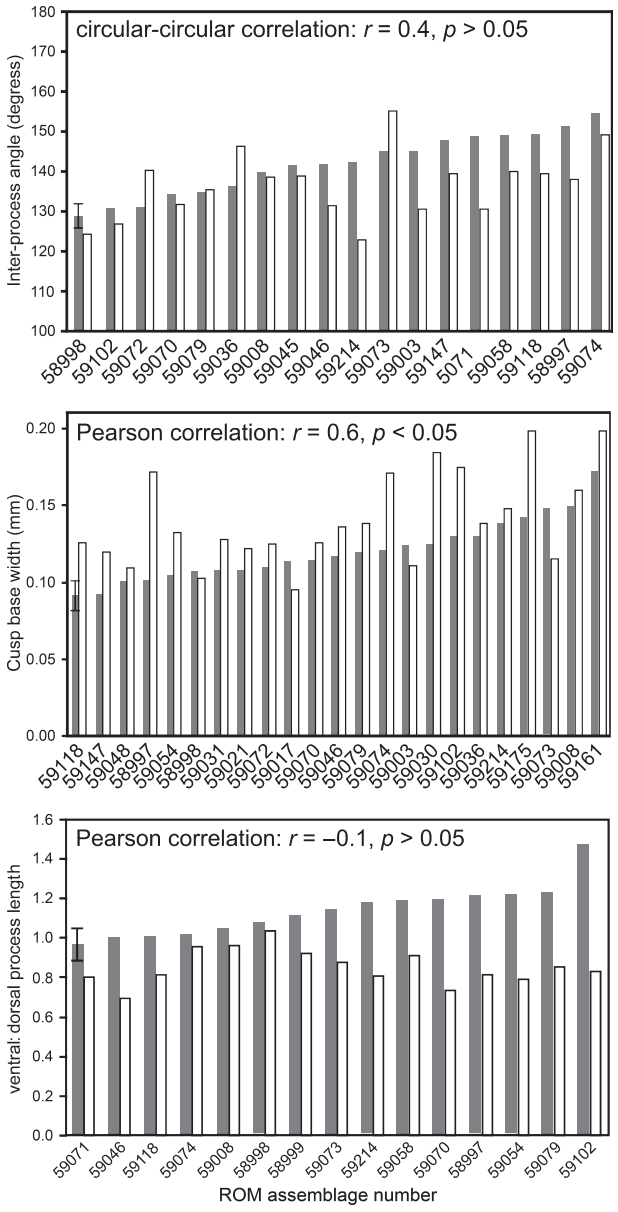

TEXT-FIG. 3. Bar charts of covariation in (A) inter-process angle, (B) cusp base width and (C) ventral/dorsal process length ratios for P elements in articulated skeletons of *W. excavata* from the Eramosa Lagerstätte. Grey bars are values for P_1 elements, white bars are values for P_2 elements. Error for each variable indicated by representative bar, calculated from spread of values produced from twelve repeat measurements by one user (DJ). Correlation statistics for each variable are provided. ROM numbers for each articulated skeleton are provided along the *x*-axis.

P element homology. The discriminatory rules are generally upheld for all characters. Text-figure 3A shows that most P_1 elements do have larger inter-process angles than the P_2 elements in each skeleton, resulting in successful discrimination of P_1 and P_2 elements in 78 per cent of articulated skeletons examined. Likewise, Text-figure 3B shows that most P_1 elements do have narrower cusp bases than P_2 elements, correctly discriminating P elements in 83 per cent of skeletons. Finally, Text-figure 3C shows the ratio of ventral/dorsal process lengths for P_1 and P_2 elements, revealing that the ratio for most P_1 elements is greater than one, indicating a relatively longer ventral process, and that for most P_2 is lower than one, indicating a relatively longer dorsal process, successfully discriminating between P elements in 100 per cent of skeletons. However, although the relative values for the characters of P_1 and P_2 elements *within* each apparatus generally support their use in traditional discrimination, Text-figure 3 clearly shows extensive individual variation in absolute character values *between* different apparatuses.

Results of correlation tests (see Text-fig. 3) indicate that within each skeleton, neither the inter-process angle (circular-circular correlation: $r = 0.4$, $p > 0.05$) nor ventral/dorsal process ratio (Pearson correlation: $r = -0.1$, $p > 0.05$) of P_1 and P_2 elements is significantly correlated. However, cusp base width did show a significant correlation (Pearson correlation: $r = 0.6$, $p < 0.05$). The low *r*-values for all three characters indicate that covariation is quite low. Moreover, the articulated skeletons sample only larger P elements; conodont elements become increasingly distinct morphologically with growth, as evidenced by the general difficulty of taxonomic assignment of small/immature specimens, even morphometrically (e.g. Girard *et al.* 2004). Mature *W. excavata* P elements might, therefore, be expected to be morphologically more distinct than juvenile individuals.

To search for a standard threshold value for dividing elements into P_1 and P_2 and to assess whether the characters are effective over a range of sizes, data for each of the three variables discussed above, derived from isolated elements and a set of 48 elements from articulated skeletons, were ordinated against total length (Text-fig. 4). The P_1 and P_2 elements from articulated skeletons do not form distinct groupings in any of the ordinations, although they do display some segregation based on ventral/dorsal process length. However, the distribution of isolated specimens appears continuous in all the plots; even for ventral/dorsal process length, they display no obvious discontinuities at which a discriminatory boundary between P_1 and P_2 elements could be drawn. These results show that, as might be expected, no single variable is an effective discriminator of P_1 and P_2 elements in isolated element collections. For P_1 and P_2 elements in articulated skeletons, however, ventral/dorsal process length provides the best single character discriminator.

Another important feature of the plots in Text-figure 4 is the small size of the isolated elements compared to the articulated specimens. The taphonomy of the Eramosa suggests that most of the elements, regardless of size, will

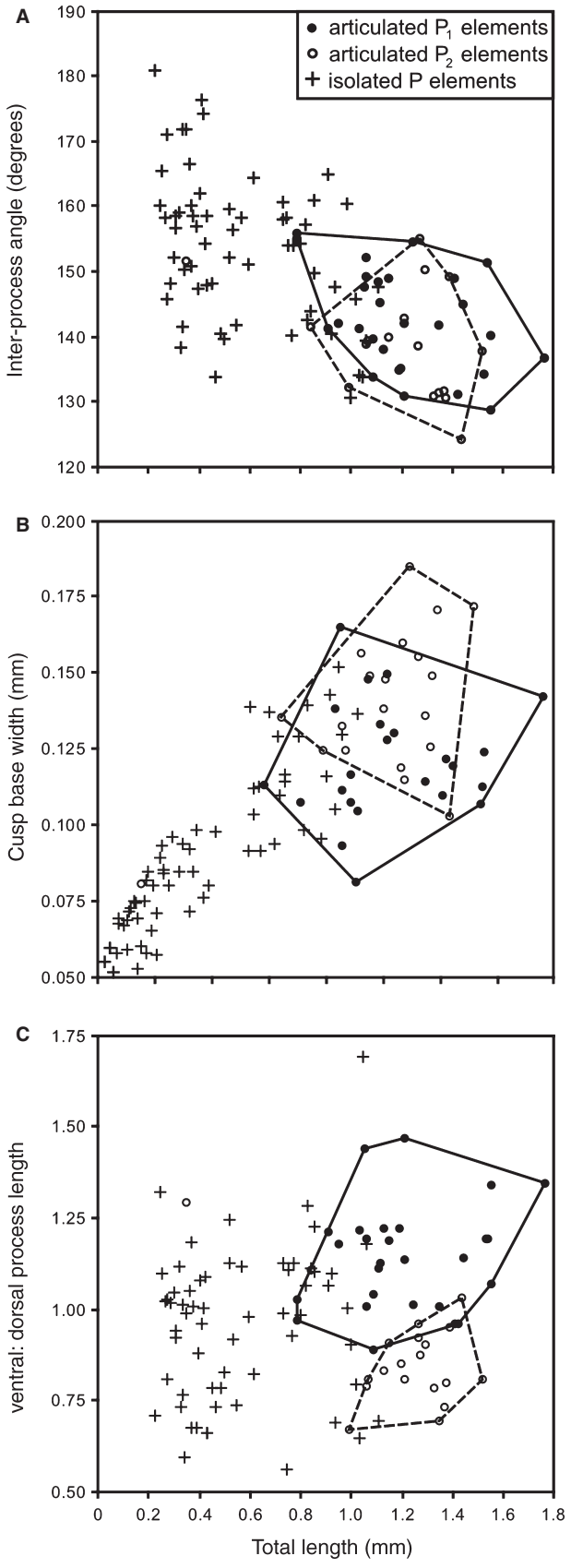

TEXT-FIG. 4. Bivariate plots of (A) inter-process angle, (B) cusp base width and (C) ventral/dorsal process length for isolated P elements and P elements from articulated skeletons of *W. excavata* from the Eramosa Lagerstätte. Measurement error is as in Text-figure 3. Convex hulls delineate P_1 and P_2 element clusters.

TABLE 1. Eigenvalues, per cent variance explained and cumulative per cent variance explained for the first two principal components from a PCA of P elements of *W. excavata* (isolated and from articulated skeletons) from the Eramosa Lagerstätte, Ontario.

PC	Eigenvalue	% Variance explained	Cumulative % variance explained
1	4.17448	41.745	41.745
2	2.26625	22.663	64.408

have been preserved within articulated skeletons (see Material and Methods). The size discontinuity, therefore, probably results from collector bias: apparatuses formed of larger elements are more easily spotted when splitting through the rock; these are removed, and any smaller apparatuses are subsequently disarticulated during dissolution of the split rock, producing the isolated elements. This is supported by the presence among the articulated skeletons of several individuals bearing elements falling within the size range of the isolated elements (DJ, pers. obs.). Unfortunately, for all but one of these, the elements are too fractured to be measured.

Principle components analysis (PCA) of articulated P elements. Articulated P_1 and P_2 elements were best separated by the first two principal components, which together account for 64.4 per cent of the variation (see Table 1 for eigenvalues and per cent variation). Text-figure 5A shows the ordination of elements in principal component morphospace based on scores for these PCs. The P_1 and P_2 elements form clear clusters, with most separation along PC-1. The plot also demonstrates that some P_1 and P_2 elements are morphometrically indistinguishable, whereas others are very different.

The inset vector diagram in Text-figure 5A illustrates which variables dominantly separate P_1 and P_2 elements. This is also shown in Table 2 as the amount of variance that each character contributes to the variance of each PC (the loading value). The greater the loading value for a character (regardless of sign), the greater is its contribution to that PC axis. Positive and negative loadings indicate whether a variable's magnitude increases or decreases in value along a PC axis.

The loading values and the inset vector diagram reveal that the variables and their directions of change do not

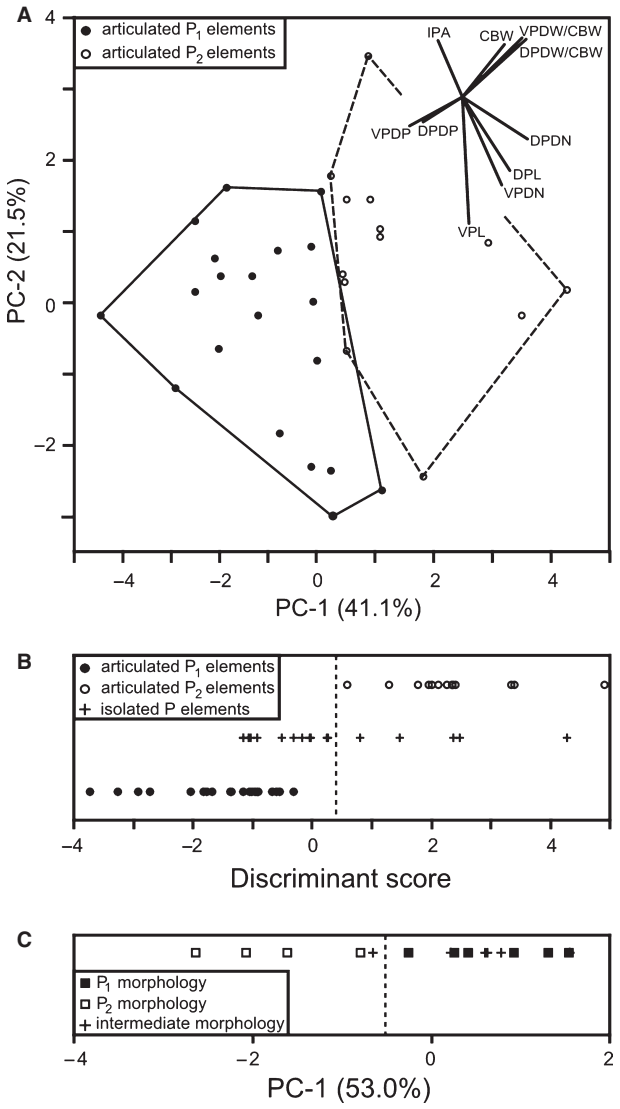

TEXT-FIG. 5. (A) Biplot ordination of articulated P elements of *W. excavata* from the Eramosa Lagerstätte on the first two principal components (PCs), based on eigenscores from PCA of ten traditional morphological variables. Convex hulls delineate P_1 and P_2 groupings. Inset illustrates vectors of variable loading relative to principal component axes. See Table 2 for vector diagram abbreviations. (B) Ordination of articulated P elements of *W. excavata* from the Eramosa Lagerstätte based on discriminant scores from a DFA of three traditional morphological variables (see text for details), with isolated elements mapped onto discriminant space of articulated P elements. Dashed line indicates whether isolated P elements were classified by the DFA as P_1 (left) or P_2 (right). (C) Ordination of isolated P elements of *W. excavata* from the Eramosa Lagerstätte on the PC-1, based on eigenscores from PCA of three traditional morphological variables. Elements are assigned to P element type based on end-members displaying clear P_1 or P_2 morphology. Dashed line indicates which P elements displaying intermediate morphologies would be classified as P_1 (right) or P_2 (left).

TABLE 2. Variable loadings on the first two principal components (PCs) from PCA of P elements of *W. excavata* (isolated and from articulated skeletons) from the Eramosa Lagerstätte, Ontario.

Variable	PC-1 loading	PC-2 loading
Ventral process length (VPL)	0.045	−0.607
Dorsal process length (DPL)	0.317	−0.344
Inter-process angle (IPA)	−0.161	0.258
Cusp base width (CBW)	0.286	0.239
Dorsal process denticle packing (DPDP)	−0.352	−0.137
Ventral process denticle packing (VPDP)	−0.256	−0.118
Cusp base width: ventral process denticle width (CBW:VPDW)	0.402	0.275
Cusp base width: dorsal process denticle width (CBW:DPDW)	0.423	0.268
Ventral process denticle number (VPDN)	0.260	−0.413
Dorsal process denticle number (DPDN)	0.438	−0.196

correspond exactly with the patterns identified and examined in the previous analyses. Ventral process length loads heavily on PC-2, reflecting the relatively longer ventral processes of P_1 elements compared to P_2. However, other characters used to qualitatively differentiate between P elements types, such as cusp size (base width), inter-process angle and dorsal process length did not contribute greatly to PC-1, along which the articulated P_1 and P_2 elements were most clearly separated. Characters relating to the denticles loaded most heavily on this axis, particularly dorsal process denticle packing and the ratio of the cusp base width to that of the dorsal process denticles.

Discriminant function analysis (DFA). The DFA of articulated elements based on traditional data assigned 100 per cent of specimens to the correct P element type (see Text-fig. 5B). Stepwise removal of variables revealed that only three were required for correct discrimination: ventral process length, the ratio of the cusp base to dorsal process average denticle base width and dorsal process denticle number. Interestingly, other characters traditionally used to differentiate P elements – cusp size, element arching and relative process lengths – appeared less effective in discriminating P elements. The morphological differences between P_1 and P_2 elements were significant, based on the three variables above (NPMANOVA: $F = 25.96$, $p < 0.05$).

The validation test, whether based on all variables or just the three identified above, correctly discriminated all the articulated P elements. Also, the DFA-based assignment of isolated elements to P_1 or P_2 categories was the same when all variables and when just the three were used.

This suggests that the DFA result is stable. When the isolated elements were projected onto the discriminant space defined by the articulated elements, they formed two clear groupings in the DFA plot (see Text-fig. 5B), one overlapping with the articulated P_1 cluster, the other with the articulated P_2 cluster. A number of elements included in the DFA had also been included in the blind expert test of articulated P elements. For these specimens, the quantitative discrimination agreed in all cases with the blind expert test for those elements where all the experts agreed on the assignment; in most cases, these were elements displaying clear end-member morphologies.

Principle components analysis (PCA) of isolated P elements. To simulate the situation where no articulated specimens are available (i.e. where the *a priori* grouping required for a DFA is not possible), a PCA of isolated specimens was conducted. This PCA was based on the three discriminating variables identified in the DFA (ventral process length, the ratio of the cusp base to dorsal process average denticle base width and dorsal process denticle number). Text-figure 5C shows isolated elements plotted along PC-1 based on scores from this PCA. When elements exhibiting clear end-member morphologies are classified qualitatively, specimens displaying more equivocal morphologies (over a third of specimens) can be assigned to P element type. This classification of intermediates also agrees with that of the DFA above.

P element discrimination based on outline data

Eigenshape (ES) analysis. Table 3 shows eigenvalues for the first ten eigenshape axes of the analysis and the per cent variance explained by each eigenshape axis. Articulated P_1 and P_2 elements were most effectively separated by ES-5 and ES-9 (although they accounted for only a small percentage of the overall shape information). Text-figure 6A shows the ordination of element outlines, based on eigenscores, in the shape space bounded by these ES axes. This figure also includes eigenshape models (hypothetical forms illustrating the pure shape variation occurring along each eigenshape axis) which serve to aid visualisation and interpretation of the shape variation associated with each axis. Shape change along ES-5 and ES-9 is subtle, but both have captured variation in the degree of curvature of the elements, with the articulated P_1 elements having a relatively straighter shape, and the articulated P_2 elements displaying a more arched profile.

The DFA of articulated elements based on scores for the first ten ES axes correctly assigned 16 of the articulated elements, a discrimination success of 94 per cent. Stepwise removal of axes revealed that only two were required to achieve the same discrimination success: ES-5 and ES-9 (see Text-fig. 6B). A significant difference was also found between P_1 and P_2 elements from articulated skeletons based on scores from ES-5 and ES-9 (NPMANOVA:

TABLE 3. Eigenvalues, per cent variance explained and cumulative per cent variance explained for the first ten eigenshape (ES) axes for P elements of *W. excavata* (isolated and from articulated skeletons) from the Eramosa Lagerstätte.

ES	Eigenvalue	% Variance explained	Cumulative % variance explained
1	21.51	91.5	91.5
2	1.13	4.8	96.3
3	0.29	1.3	97.6
4	0.14	0.6	98.2
5	0.08	0.4	98.5
6	0.07	0.3	98.8
7	0.05	0.2	99.1
8	0.05	0.2	99.2
9	0.04	0.2	99.4
10	0.03	0.1	99.6

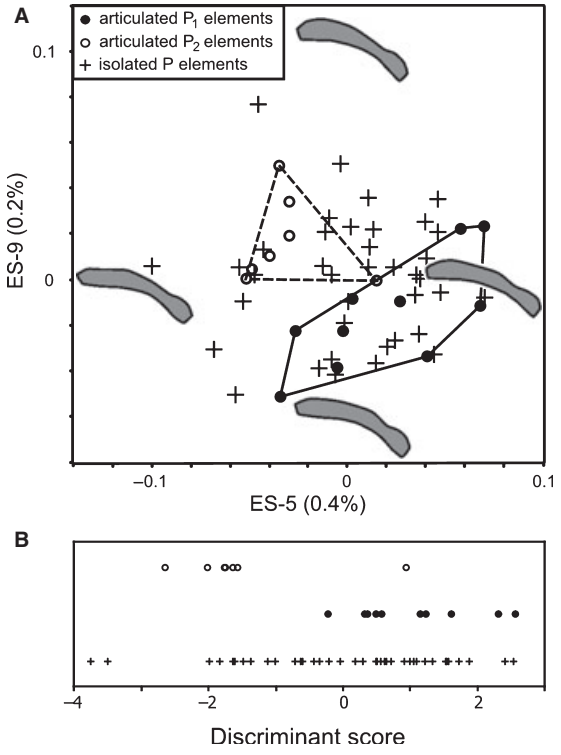

TEXT-FIG. 6. (A) Ordination of P elements of *W. excavata* (isolated and from articulated skeletons) from the Eramosa Lagerstätte on eigenshape (ES) axes five and nine, based on eigenshape scores. Outlines represent end-member shape models of shape change along each axis. Convex hulls delineate P_1 and P_2 element clusters. (B) Ordination of articulated P elements of *W. excavata* from the Eramosa Lagerstätte, based on discriminant scores from a DFA of ES-5 and ES-9 scores, with isolated specimens mapped onto the discriminant space of articulated P elements.

$F = 9.658$, $p < 0.05$). The validation test, whether based on scores for all axes or just ES-5 and ES-9, correctly assigned 16 (94 per cent) of the articulated elements. However, the assignment of isolated specimens when all variables were included and when only ES-5 and ES-9 were included concurred in only 60 per cent of cases, suggesting that a DFA will produce inconsistent results depending on which variables are included.

Fourier analysis. Table 4 shows eigenvalues for the first ten principal components (PCs) from the PCA of elliptic Fourier coefficients and the per cent variance explained by each. The articulated P_1 and P_2 elements were most clearly separated on PC-3 and PC-10. Text-figure 7A shows the ordination of element outlines, based on PC scores, in the shape space bounded by these PC axes. End-member elements and their outlines are figured to aid visualisation and interpretation of the shape variation. As in the ES analysis, degree of element curvature appears to be the most obvious variation, with P_2 elements being relatively more arched than P_1 elements.

The DFA of articulated elements based on coefficients for the first eight elliptic Fourier harmonics correctly assigned 100 per cent of the articulated elements (see Text-fig. 7B). Stepwise removal of coefficients revealed that only the second and the third were required to achieve the same discrimination success. A significant difference was also found between P_1 and P_2 elements from articulated skeletons based on coefficients two and three (NPMANOVA: $F = 9.658$, $p < 0.05$). The validation test, whether based on scores for all axes or just the second and third coefficient, correctly assigned 100 per cent of the articulated elements. However, the assignment of isolated elements to P_1 or P_2 categories using the discriminant function derived from articulated elements based on all harmonics or just coefficients two and three, concurred in only 55 per cent of cases. As for the ES analysis, this indicates that a DFA will not produce consistent results when different variables are included.

TABLE 4. Eigenvalues, per cent variance explained and cumulative per cent variance explained for first ten principle components (PCs) from PCA of Fourier coefficients for P elements of *W. excavata* (isolated and from articulated skeletons) from the Eramosa Lagerstätte.

PC	Eigenvalue	% Variance explained	Cumulative % variance explained
1	0.0030	33.9	33.9
2	0.0015	16.3	50.1
3	0.0010	11.5	61.6
4	0.0008	9.3	70.9
5	0.0005	6.1	77.0
6	0.0005	5.3	82.3
7	0.0004	4.0	86.3
8	0.0002	2.8	89.1
9	0.0002	2.5	91.6
10	0.0002	2.3	93.9

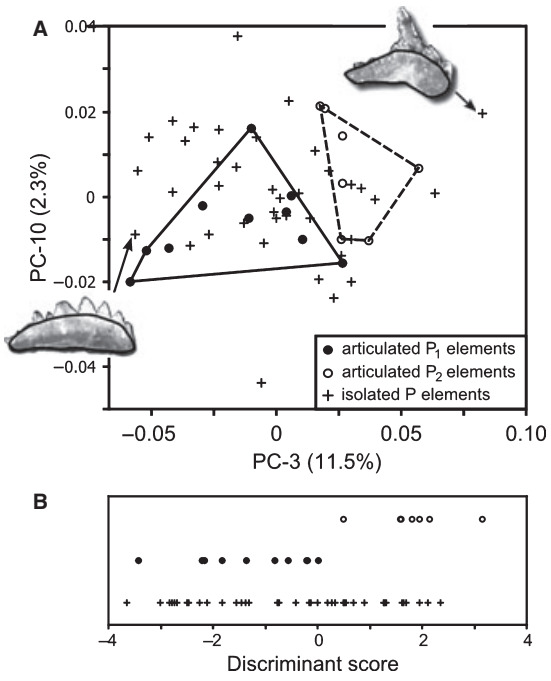

TEXT-FIG. 7. (A) Ordination of P elements of *W. excavata* (isolated and from articulated skeletons) from the Eramosa Lagerstätte on principal component (PC) axes one and three, based on PC scores from a PCA of Fourier coefficients produced by an EFA. End-member morphologies for each axis are illustrated by outlines superimposed on images of elements they represent. Convex hulls delineate P_1 and P_2 element clusters. (B) Ordination of P elements of *W. excavata* from the Eramosa Lagerstätte, based on discriminant scores from DFA of Fourier coefficients from the first eight harmonics, with isolated specimens mapped onto the discriminant space of articulated P elements.

DISCUSSION AND CONCLUSIONS

Assignment of isolated specimens by discriminant function analysis (DFA) of scores from the principal components analysis of traditional variables concurs with assignment by DFA of eigenshape scores in 86 per cent of cases, and with the DFA of principal component scores from the principle components analysis of Fourier coefficients in 100 per cent of cases. The DFA based on scores from the two outline analyses concurred in 71 per cent of cases. Because eigenshape analysis is more sensitive than elliptic Fourier analysis (Rohlf 1986; Haines and Crampton 2000), broad changes in element curvature may have been swamped by smaller-scale shape variation in the for-

mer, which may explain the weaker separation of articulated P elements by the DFA of eigenscores. The smaller number of articulated elements relative to isolated specimens available for the outline analyses may explain the generally poorer performance of these data in allowing reliable discrimination between P_1 and P_2 elements.

Based on these results, we conclude that a PCA of three traditional morphometric variables (ventral process length, the ratio of the cusp base to dorsal process average denticle base width and dorsal process denticle number) offers the most effective morphometric tool for recognising homology in isolated elements of *W. excavata* from morphological criteria alone. The success rate of the method compares favourably with expert identification yet requires little *a priori* experience of the taxon. Moreover, because only three variables need to be measured, data acquisition and analysis should be relatively quick.

Because the morphometric measurements are standardised, the methodology presented here also holds promise of broad application to other conodont taxa where morphologically similar elements occupy different locations within the skeleton; for example in many prioniodinins (*sensu* Purnell and Donoghue 2005; Donoghue *et al.* 2008), where elements may display even greater morphological similarity than that manifested in *W. excavata* from the Eramosa Lagerstätte. As demonstrated above, isolated specimens displaying clear end-member morphologies could be used to identify the different element fields in those taxa lacking preserved articulated skeletons.

Increasing the reliability of hypotheses of primary homology using these protocols will allow more rigorous cladistic analyses of conodonts, enable us to derive a clearer picture of morphological evolution of different element types within the conodont skeleton and allow us to draw more accurate palaeoecological conclusions (such as census counts) from collections of isolated specimens. Moreover, the ability of the methodology to determine quantitatively which variables discriminate between morphologically similar elements, providing more objective justification for selecting diagnostic characters, has obvious utility not only in establishing element homology, but also in taxonomy. The methodology will also aid in establishing more accurate taxonomic boundaries by reducing the artificially inflated estimates of variation within different elements types resulting from incorrectly including P_1 among P_2 elements, and vice versa.

Although the multivariate analyses identified significant differences between P_1 and P_2 elements in *W. excavata*, they also quantify the qualitative observation that individuals vary in the degree of morphological differentiation between P_1 and P_2 elements within skeletons: some individuals posses P_1 and P_2 elements that are obviously different, some that are remarkably similar. Yet poorly and well-differentiated P elements appear to represent end-members of a smooth continuum. This reflects a general morphological flexibility within and between the structural components of P elements. The adaptive significance of this variation, which presumably reflects the degree of functional differentiation of the two P element pairs, represents an important area for further research into developmental plasticity, specialisation and functionality within these earliest vertebrate feeding structures.

Acknowledgements. We thank those conodont workers who were brave enough to put their expertise to the test in our blind analysis of qualitative assessment of element homologies in *W. excavata*. We are grateful to Peter Roopnarine and Norm MacLeod for their reviews of the manuscript. The comments of Richard J. Aldridge on earlier versions of the manuscript were also most helpful. The funding of NERC (Studentship NER/S/A/2002/10486 to DOJ, Advanced Fellowship NER/J/S/2002/00673 to MAP) and fieldwork funding by the ROM's Department of Natural History to PvB are gratefully acknowledged.

REFERENCES

ATCHLEY, W. R., GASKINS, C. T. and ANDERSON, D. 1976. Statistical properties of ratios. I. Empirical results. *Systematic Zoology*, **25**, 137–148.

BARNES, C. R., KENNEDY, D. J., MCCRACKEN, A. D., NOWLAND, G. S. and TARRANT, G. A. 1979. Structure and evolution of Ordovician conodont apparatuses. *Lethaia*, **12**, 125–151.

BRANSON, E. B. and MEHL, M. G. 1933. Conodonts from the Bainbridge (Silurian) of Missouri. *University of Missouri Studies*, **8**, 39–53.

CRAMPTON, J. S. 1995. Elliptic Fourier shape-analysis of fossil bivalves – some practical considerations. *Lethaia*, **28**, 179–186.

—— and HAINES, A. J. 1996. Users' manual for programs HANGLE, HMATCH, and HCURVE for the Fourier shape analysis of two-dimensional outlines. *Institute of Geological & Nuclear Sciences science report*, **96/37**, 28.

CRONIER, C., RENAUD, S., FEIST, R. and AUFFRAY, J. C. 1998. Ontogeny of *Trimerocephalus lelievrei* (Trilobita, Phacopida), a representative of the Late Devonian phacopine paedomorphocline: a morphometric approach. *Paleobiology*, **24**, 359–370.

DONOGHUE, P. C. J., PURNELL, M. A., ALDRIDGE, R. J. and ZHANG, S. 2008. The interrelationships of complex conodonts (Vertebrata). *Journal of Systematic Palaeontology*, **6**, 119–153.

FERSON, S., ROHLF, F. J. and KOEHN, R. K. 1985. Measuring shape variation of two-dimensional outlines. *Systematic Zoology*, **34**, 59–68.

GIARDINA, C. R. and KUHL, F. P. 1977. Accuracy of curve approximation by harmonically related vectors with elliptical loci. *Computer Graphics and Image Processing*, **6**, 277–285.

GIRARD, C., RENAUD, S. and SÉRAYET, A. 2004. Morphological variation of *Palmatolepis* Devonian conodont: species versus genera. *Comptes Rendus Palevol*, **3**, 1–8.

HAINES, A. J. and CRAMPTON, J. S. 2000. Improvements to the method of Fourier shape analysis as applied in morphometric studies. *Palaeontology*, **43**, 765–783.

HAMMER, Ø., HARPER, D. A. T. and RYAN, P. D. 2001. PAST: paleontological statistics software package for education and data analysis. *Palaeontologia Electronica*, **4**, Article 4.

HAWKINS, J. A., HUGHES, C. E. and SCOTLAND, R. W. 1997. Primary homology assessment, characters and character states. *Cladistics*, **13**, 275–283.

JEPPSSON, L. 1969. Notes on some Upper Silurian multielement conodonts. *Geologiska Föreningens I Stockholm Förhandlingar*, **91**, 12–24.

——1974. Aspects of Late Silurian conodonts. *Fossils and Strata*, **6**, 1–54.

——ANEHUS, R. and FREDHOLM, D. 1999. The optimal acetate buffered acetic acid technique for extracting phosphatic fossils. *Journal of Paleontology*, **73**, 964–972.

JONES, D. O. and PURNELL, M. A. 2007. A new semi-automatic morphometric protocol for conodonts and a preliminary taxonomic application. 239–259. *In* MACLEOD, N. (ed.). *Automated object identification in systematics: theory, approaches, and applications*. CRC Press (for Systematics Association), London, 339 pp.

KUHL, F. P. and GIARDINA, C. R. 1982. Elliptic Fourier features of a closed contour. *Computer Graphics and Image Processing*, **18**, 236–258.

LOHMANN, G. P. 1983. Eigenshape analysis of micro-fossils – a general morphometric procedure for describing changes in shape. *Journal of the International Association for Mathematical Geology*, **15**, 659–672.

—— and SCHWEITZER, P. N. 1990. On eigenshape analysis. 145–166. *In* ROHLF, F. J. and BOOKSTEIN, F. L. (ed.). *Michigan morphometric workshop*. The Univeristy of Michigan Museum of Geology, The University of Michigan, Ann Arbor, Michigan, 396 pp.

MACLEOD, N. 1999. Generalizing and extending the eigenshape method of shape visualization and analysis. *Paleobiology*, **25**, 107–138.

—— and ROSE, K. D. 1993. Inferring locomotor behaviour in Paleogene mammals via eigenshape analysis. *American Journal of Science*, **293-A**, 300–355.

MARCUS, L. F. 1990. Traditional morphometrics. 77–122. *In* ROHLF, F. J. and BOOKSTEIN, F. L. (ed.). *Michigan Morphometric Workshop*. The University of Michigan Museum of Zoology, Ann Arbor, MI, 396 pp.

MERRILL, G. K. and MERRILL, S. M. 1974. Pennsylvanian nonplatform conodonts, IIa: The dimorphic apparatus of *Idioprioniodus*. *Geologica et Palaeontologica*, **8**, 119–130.

PURNELL, M. A. 1993. The *Kladognathus* apparatus (Conodonta, Carboniferous) – Homologies with Ozarkodinids, and the Prioniodinid Bauplan. *Journal of Paleontology*, **67**, 875–882.

—— and DONOGHUE, P. C. J. 1998. Skeletal architecture, homologies and taphonomy of ozarkodinid conodonts. *Palaeontology*, **41**, 57–102.

————2005. Between death and data: Biases in interpretation of the fossil record of conodonts. 7–25. *In* PURNELL, M. A. and DONOGHUE, P. C. J. (eds). Special Papers in Palaeontology Series, *Conodont biology and phylogeny: interpreting the fossil record*. Palaeontological Association, London, 218 pp.

———— and ALDRIDGE, R. J. 2000. Orientation and anatomical notation in conodonts. *Journal of Paleontology*, **74**, 113–122.

ROHLF, F. J. 1986. Relationships among eigenshape analysis, Fourier analysis, and analysis of coordinates. *Mathematical Geology*, **18**, 845–854.

——2003. tpsDIG. Version 1.37.

VON BITTER, P. H. and PURNELL, M. A. 2005. An experimental investigation of post-depositional taphonomic bias in conodonts. 39–56. *In* PURNELL, M. A. and DONOGHUE, P. C. J. (eds). Special Papers in Palaeontology, *Conodont Biology and Phylogeny: interpreting the fossil record*. Palaeontological Association, London, 218 pp.

————TETRAULT, D. K. and STOTT, C. A. 2007. Eramosa Lagerstätte – exceptionally preserved soft-bodied biotas with shallow-marine shelly and bioturbating organisms (Silurian, Ontario, Canada). *Geology*, **35**, 879–882.

WALLISER, O. H. 1964. Conodonten des Silurs. *Abhandlungen der Hessischen Landesamtes Bodenforschung*, **41**, 1–106.

APPENDIX

Multivariate morphometric measurement data for Wurmiella excavata P elements from the Eramosa Lagerstätte

Data for articulated P_1 elements

ROM number	Side (sinistral/dextral)	VPL (mm)	DPL (mm)	IPA (degrees)	CBW (mm)	DPDP	VPDP	VPDN	DPDN
58992	S	0.5763	0.4825	152.1	0.1159	15.3	10.1	6	7
58997	S	0.8392	0.7037	151.4	0.1118	15.1	13	11	11
58998	D	0.8035	0.7499	128.8	0.1070	15.2	12.2	10	11

Data for articulated P_1 elements

ROM number	Side (sinistral/dextral)	VPL (mm)	DPL (mm)	IPA (degrees)	CBW (mm)	DPDP	VPDP	VPDN	DPDN
58999	D	0.5838	0.5235	148.5	0.1127	14.2	16.1	9	7
59003	D	0.5911	0.5243	145.2	0.1243	14.6	15.4	9	8
59008	S	0.5556	0.5322	139.8	0.1496	13	14.8	8	7
59071	S	0.5004	0.4128	141.2	0.1136	14.9	13.2	7	6
59031	D	0.6222	0.5085	138.2	0.1076	14.6	13.8	9	7
59046	S	0.6787	0.6727	141.7	0.1169	10.4	10.6	7	7
59047	?	0.5647	0.4876	143	0.1085	15.7	12.6	9	7
59054	S	0.5661	0.4650	141.3	0.1049	15.2	11.9	7	7
59070	S	0.8329	0.6990	134.3	0.1146	17	13.1	11	12
59072	S	0.6976	0.7250	131.1	0.1099	13.6	11.6	8	10
59073	?	0.7709	0.6759	145.1	0.1478	14.6	10	8	10
59074	S	0.6259	0.6174	154.6	0.1216	11.8	11.2	7	7
59079	S	0.6552	0.5352	135	0.1197	17.5	12.3	8	9
59102	?	0.7220	0.4916	130.8	0.1303	13.3	9.7	7	7
59147	D	0.6206	0.4312	147.8	0.0933	10.9	11.4	7	5
59175	S	0.8905	0.6645	140.3	0.1424	13	10.8	10	9
59214	S	0.6453	0.5686	142.2	0.1384	13.1	9.7	6	7

Data for articulated P_2 elements

ROM number	Side (sinistral/dextral)	VPL (mm)	DPL (mm)	IPA (degrees)	CBW (mm)	DPDP	VPDP	VPDN	DPDN
58997	S	0.6807	0.8396	137.9	0.1722	16.3	14	10	14
58998	S	0.7297	0.7074	124.2	0.1031	19.6	14.7	11	14
59008	D	0.6220	0.6467	138.6	0.1599	16.4	11.1	7	11
59020	D	0.4441	0.4009	141.6	0.1353	20.1	16	7	8
59030	?	0.6154	0.6803	150.3	0.1849	13.2	10.6	7	9
59070	S	0.5795	0.7888	131.6	0.1259	13.8	13.4	8	11
59071	?	0.6108	0.7651	130.6	0.1494	19.7	17.7	11	15
59073	D	0.5947	0.6806	155.2	0.1151	17.8	13.4	8	12
59074	S	0.6796	0.7130	149.2	0.1712	17.3	14	10	12
59079	D	0.5525	0.6484	135.3	0.1383	16.9	13.5	7	11
59102	S	0.5822	0.7436	131	0.1554	14.9	9.9	6	11
59118	S	0.4780	0.5896	139.4	0.1248	17.6	13.5	6	10
59214	?	0.5395	0.6687	142.9	0.1481	17.3	11.3	6	12

Data for isolated P elements

ROM number	Side (sinistral/dextral)	VPL (mm)	DPL (mm)	IPA (degrees)	CBW (mm)	DPDP	VPDP	VPDN	DPDN
58941	D	0.4501	0.5676	145.7	0.1430	16.7	11.6	5	9
58945	D	0.4925	0.4900	160.4	0.0955	16.5	12.2	6	8
58947	S	0.3940	0.3557	154.1	0.1036	16.2	12.5	5	6
58958	S	0.4561	0.6546	147.7	0.1366	15.1	10.2	5	10
58968	S	0.4091	0.3627	154.1	0.0917	17.1	17.3	7	6
56355	D	0.4487	0.4070	149.7	0.1146	13.2	13.9	6	5
56363	D	0.4667	0.3630	142.7	0.1295	16.1	13	6	6
58971	D	0.4064	0.6288	134.2	0.1055	19.7	14.6	6	12
59233	S	0.4219	0.3961	157.2	0.0938	15.6	15.5	7	6
59234	S	0.3990	0.4047	154.4	0.1374	13.5	12.3	5	5
56365	S	0.4855	0.4409	140.4	0.0986	13.8	10.8	5	6

Data for isolated P elements

ROM number	Side (sinistral/dextral)	VPL (mm)	DPL (mm)	IPA (degrees)	CBW (mm)	DPDP	VPDP	VPDN	DPDN
59240	S	0.3691	0.3982	140.2	0.1127	17.1	16.2	6	7
59244	S	0.5739	0.4865	139.4	0.1297	13.6	12.7	7	7
59249	?	0.4683	0.4394	165	0.1293	13.3	11.2	5	6
59250	S	0.5269	0.6313	150.1	0.1085	12.2	10.7	7	7
56364	S	0.4421	0.3977	144	0.1101	15.2	13.8	7	7